

Polynuclear Complex Family of Cobalt(II)/Sulfonylcalixarene: One-Pot Synthesis of Cluster Salt $[\text{Co}_{14}]^+[\text{Co}_4]^-$ and Field-Induced Slow Magnetic Relaxation in a Six-Coordinate Dinuclear Cobalt(II)/Sulfonylcalixarene Complex

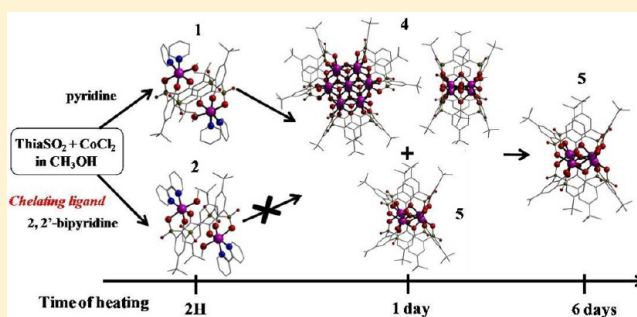
Meriem Lamouchi,[†] Erwann Jeanneau,[†] Ghenadie Novitchi,[‡] Dominique Luneau,[†] Arnaud Brioude,[†] and Cédric Desroches^{*,†}

[†]Laboratoire des Multimatériaux et Interfaces (UMR 5615), Université Claude Bernard Lyon 1, Campus de La Doua, 69622 Villeurbanne Cedex, France

[‡]Laboratoire National des Champs Magnétiques Intenses, CNRS, 38042 Grenoble, France

S Supporting Information

ABSTRACT: In this paper, we report the synthesis and description of a new family of polynuclear cobalt(II) complexes. Starting from the same initial compounds but varying the reaction time results in the formation of several new clusters, an original structure based on $[\text{Co}_{14}][\text{Co}_4]$ clusters was obtained, representing the first one-pot synthesis of a cobalt aggregate salt reported in the literature. The synthesis and magnetic properties of these cobalt compounds are discussed. Three of them display a binuclear molecular structure (1–3) with two encapsulated Co^{II} ions and show slow relaxation of magnetization at small applied magnetic field ($U_{\text{eff}} = 10.7$ K for 2 and $U_{\text{eff}} = 20.3$ K for 3), a characteristic of single-molecule-magnet materials.



INTRODUCTION

Over the past decades, extensive research in the field of polynuclear metallic complex synthesis has been conducted, mostly led by the discovery of magnetic relaxation and spin tunneling at low temperature in large-spin molecular systems. These metallic complexes, so-called single-molecule magnets (SMMs), attracted major attention to advance the understanding of the origin, control, and improvement of their magnetic properties as prospective magnetic materials.^{1,2} Some promising approaches to increase the energy barrier of magnetization relaxation have been suggested, such as enhancing the global anisotropy of the polynuclear molecular entities by combining anisotropic building blocks possessing some obvious metal ions.³ The Co^{II} ion is a good candidate because of its strong orbital contribution to the magnetic moment and thus to its strong magnetic anisotropy.⁴ Nevertheless, orbital angular momentum of Co^{II} implies complexity of modeling the magnetic behavior, even for binuclear species.⁵ Among the various Co^{II} -based clusters, in particular those with high nuclearity, only a few of them are known to display SMM behavior.⁶

In order to prepare these types of molecular complexes, we need to control many aspects of the polynuclear complex structures, including the nuclearity of the metallic ion, the position of the ions with respect to each other, the geometry,

and the coordination number of all ions. The so-called “molecular paneling” and “serendipitous assembly” approaches are two strategies to synthesize polynuclear complexes of the type $[\text{M}_x(\mu\text{-L})_y\text{L}'_z]^n$, where M is the metal ion, $\mu\text{-L}$ a bridging ligand, L' a terminal ligand (monodentate or chelating), and n the charge of the complex.⁷ Often “serendipitous assembly” is the starting point. Indeed, control of the number and coordination mode of bridging ligands, such as oxo, hydroxo, or carbonato, or also multidentate terminal ligands complicates the design and control of such assemblies.⁸ Furthermore, concerning solvothermal synthesis, the fact that these molecular compounds are prepared and crystallized from a one-pot reaction does not simplify things.

The choice of the terminal ligand is crucial in order to limit metallic polycondensation, to control a part of the coordination sphere, and to protect polynuclear metallic cores with an organic outer shell. Generally, if one aggregate is obtained, whether it is predicted or not, this can provide a basic building block or magnetic molecule that can then be further exploited.

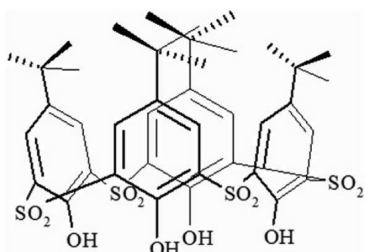
The family of calix[4]arene macrocycles has recently emerged as multidentate ligands for polynuclear metal cluster formation.^{9,10} Our previous studies in this field were mostly

Received: May 17, 2013

Published: December 23, 2013

focused on the macrocyclic thiacalixarene group and, in particular, sulfonylthiacalixarenes.^{9b,c} The compound *p*-tert-butylsulfonylthiacalixarene (ThiaSO₂), an oxidized derivative of thiacalix[4]arene, is composed of four phenolic groups linked by sulfonyl functions that are able to complex and bridge a variety of metals (Scheme 1).⁹

Scheme 1. Representation of ThiaSO₂ in the Cone Conformation



ThiaSO₂ is usually multichelating because of the proximity of the phenolic and sulfonyl oxygen atoms, which have different binding modes; each binding mode usually depends on the macrocycle conformation. Very few examples of mononuclear complexes with this macrocycle, oxidized or not, can be found in the literature.¹² [4.22221111] (Harris notation¹³) mode, where the four phenolato oxygen atoms are μ and one oxygen atom of each sulfonyl group is coordinated, is generally encountered with a cone conformation and leads to a tetranuclear metallic structure called “tail-to-tail” perfect or shifted.^{9b–c} 2[1.111] binding mode, where two phenolato oxygen atoms and one sulfonyl group oxygen atom are coordinated, is mainly observed for the 1,2 alternate conformation.^{9m} Note that the 1,2 alternate conformation for *p*-tert-butylthiacalix[4]arene or *p*-tert-butylsulfonylcalix[4]arene (ThiaSO₂) has never been obtained under solvothermal conditions. A variety of clusters involving metal cations and the sulfonylcalix[4]arene macrocycle have been reported; complexes of ThiaSO₂ with Co^{II} ions are the most described in the literature.^{9g–m} It is specifically with this type of ion that the largest metallic aggregates with thiacalixarene were obtained.^{9g,h} The nuclearities of these clusters have been reported as between 2 and 32 atoms of cobalt. Their syntheses are realized at atmospheric or autogenous pressure (solvothermal conditions), but few details about variation of the synthesis parameters such as the pH, solvent temperature, atmosphere, metal-to-ligand ratio, or concentration are given.

In the present work, we report the synthesis and characterization of a new family of polynuclear cobalt(II) complexes. Using the same initial compound and with a change in the reaction time, several clusters have been synthesized. The magnetic properties of these cobalt compounds are also discussed.

EXPERIMENTAL SECTION

All chemicals and solvents were used as received (solvents, Carlo Erba RPE; chemicals, Aldrich); all preparations and manipulations were performed under aerobic conditions. The ligands *p*-tert-butylthiacalix[4]arene (ThiaS) and *p*-tert-butylsulfonylcalix[4]arene (ThiaSO₂) were synthesized according to published procedures.¹⁰ Fourier transform infrared (FTIR) spectra were recorded on a SAFAS (FTIR-ATR) spectrometer. Mass spectra were performed on a MicroTOF-QII Bruker mass spectrometer [electrospray ionization (ESI) source].

Synthesis of [Co₂(ThiaSO₂)(pyridine)₄(CH₃OH)₂] (1). Red single crystals of **1** were obtained from the reaction of a mixture of ThiaSO₂ (0.07 g, 0.082 mmol), CoCl₂·6H₂O (0.04 g, 0.19 mmol), pyridine (0.3 mL, 3.7 mmol), CH₃OH (10 mL), and H₂O (2 mL) in a 20 mL Teflon-lined autoclave, which was kept at 170 °C under autogenous pressure for 2 h, then slowly cooled to 20 °C at 7 °C/h, and kept at room temperature for 1 day. Yield: 35%. Anal. Calcd for C₆₂H₇₂O₁₄N₄S₄Co₂ (*M* = 1343.4 g/mol): C, 55.43; H, 5.40. Found: C, 55.21; H, 5.38. IR (cm⁻¹): 3588 (w), 3512 (w), 2959 (m), 2905 (w), 2868 (w), 1604 (s), 1488 (s), 1459 (s), 1447 (s), 1395 (w), 1363 (m), 1337 (w), 1261 (s), 1219 (w), 1194 (w), 1152 (w), 1119 (m), 1071 (s), 1042 (m), 1011 (w), 930 (w), 905 (m), 842 (m), 803 (s), 757 (s), 698 (s), 663 (w), 629 (s), 608 (s).

Synthesis of [Co₂(ThiaSO₂)(2,2'-bipyridine)₂(CH₃OH)₂] (2). Yellow single-crystalline needles of **2** were obtained from the reaction of a mixture of ThiaSO₂ (0.07 g, 0.082 mmol), CoCl₂·6H₂O (0.04 g, 0.19 mmol), pyridine (0.05 mL, 0.62 mmol), 2,2'-bipyridine (0.1 g, 0.64 mmol), CH₃OH (10 mL), and H₂O (1 mL) in a 20 mL Teflon-lined autoclave, which was kept at 170 °C under autogenous pressure for 2 h and then slowly cooled to 20 °C at 7 °C/h. The crystals were isolated upon filtration and washed with methanol. Yield: 60–70%. Anal. Calcd for C₆₂H₆₈O₁₄N₄S₄Co₂ (*M* = 1339.4 g/mol): C, 55.59; H, 5.11. Found: C, 55.35; H, 5.05. IR (cm⁻¹): 3360 (w), 2959 (m), 2909 (w), 2869 (w), 1600 (m), 1577 (w), 1487 (m), 1473 (m), 1443 (m), 1363 (w), 1310 (s), 1262 (s), 1221 (w), 1158 (s), 1132 (s), 1081 (s), 1020 (w), 904 (m), 836 (w), 793 (s), 760 (s), 738 (m), 634 (s), 619 (s).

Synthesis of [Co₂(ThiaSO₂)(en)₂(pyridine)₂] (3). Orange-brown single crystals of **3** were obtained from the reaction of a mixture of ThiaSO₂ (0.07 g, 0.082 mmol), CoCl₂·6H₂O (0.04 g, 0.19 mmol), pyridine (0.05 mL, 0.62 mmol), ethylenediamine (0.05 mL, 0.75 mmol), CH₃OH (10 mL), and H₂O (1 mL) in a 20 mL Teflon-lined autoclave, which was kept at 170 °C under autogenous pressure for 2 h and then slowly cooled to 20 °C at 7 °C/h. The crystals were isolated upon filtration and washed with methanol. Yield: 60–70%. Anal. Calcd for C₅₄H₇₀O₁₂N₆S₄Co₂ (*M* = 1241.31 g/mol): C, 52.25; H, 5.68. Found: C, 52.18; H, 5.70. IR (cm⁻¹): 3507 (w), 3352 (w), 3289 (w), 2955 (m), 2907 (w), 2868 (w), 1600 (s), 1490 (s), 1464 (w), 1395 (w), 1362 (m), 1327 (w), 1258 (s), 1215 (w), 1193 (w), 1117 (s), 1069 (s), 1033 (m), 1009 (w), 993 (m), 840 (m), 799 (s), 760 (s), 629 (m), 609 (s).

Synthesis of [Co₁₄(ThiaSO₂)₃(μ₄-OH)₃(μ₆-O)₃(OCH₃)₆]{Co₄(ThiaSO₂)₂(μ₄-OH)}⁻] (4). Purple rectangular-parallelepiped single crystals of **4** were obtained from the reaction of a mixture of ThiaSO₂ (0.07 g, 0.082 mmol), CoCl₂·6H₂O (0.07 g, 0.33 mmol), pyridine (0.3 mL, 3.7 mmol), CH₃OH (10 mL), and H₂O (1 mL) in a 20 mL Teflon-lined autoclave, which was kept at 170 °C under autogenous pressure for 36 h, then slowly cooled to 20 °C at 7 °C/h, and kept at room temperature for 1 day. Sample **4** is polluted with compound **5**. The crystals were isolated upon filtration and washed with methanol, and the crystals **B** of large sizes are sorted out under a microscope. Yield: 20%. ESI-MS (positive mode). Calcd for [C₁₂₆H₁₅₃O₄₈S₁₂Co₁₄]: *m/z* 3645. Found: *m/z* 3575, 3589, 3603, 3617 (Figures S8 and S9 in the Supporting Information, SI). ESI-MS (negative mode). Calcd for [C₈₀H₈₉O₂₅S₈Co₄]: *m/z* 1941. Found: *m/z* 1941.1 (Figure S10 in the SI). IR (cm⁻¹): 2962 (m), 2907 (w), 2871 (w), 1603 (m), 1525 (w), 1464 (s), 1398 (w), 1364 (w), 1321 (w), 1309 (s), 1293 (w), 1260 (s), 1199 (w), 1132 (s), 1082 (s), 1019 (m), 836 (m), 798 (s), 742 (m), 705 (w), 627 (s).

Synthesis of [Co₄(HThiaSO₂)₂(μ₄-OH)] (5). Brown prismatic single crystals of **5** were obtained from the reaction of a mixture of ThiaSO₂ (0.07 g, 0.082 mmol), CoCl₂·6H₂O (0.07 g, 0.33 mmol), pyridine (0.3 mL, 3.7 mmol), CH₃OH (10 mL), and H₂O (1 mL) in a 20 mL Teflon-lined autoclave, which was kept at 170 °C under autogenous pressure for 6 days, then slowly cooled to 20 °C at 7 °C/h, and kept at room temperature for 1 day. The crystals were isolated upon filtration and washed with methanol. Yield: 55%. ESI-MS (negative mode). Calcd for [C₈₀H₈₉O₂₅S₈Co₄]: *m/z* 1941 (*M* - H). Found: *m/z* 1941.1 (Figures S12 and S13 in the SI).

Table 1. Selected Crystal Data and Structure Refinement Parameters of 1–5

	1	2	3	4	5
formula	C ₆₂ H ₇₂ Co ₂ N ₄ O ₁₄ S ₄	C ₆₁ H ₆₃ Co ₂ N ₄ O ₁₄ S ₄	C ₅₄ H ₆₂ Co ₂ N ₆ O ₁₂ S ₄	C ₂₀₆ H ₂₄₂ Co ₁₈ O ₇₃ S ₂₀	C ₈₀ H ₈₈ Co ₄ O ₂₅ S ₈
M/(g/mol)	1343.38	1322.29	1233.24	5352.51	1941.82
T/K	150	150	100	150	100
λ/Å	0.7107	0.7107	0.7107	0.7107	0.7107
cryst syst	monoclinic	monoclinic	monoclinic	orthorhombic	monoclinic
space group	P2 ₁ /n	P2 ₁ /n	P2 ₁ /c	Pbma	P2 ₁ /n
a/Å	12.763(2)	12.310(3)	11.9696(9)	22.5565(8)	22.813(1)
b/Å	19.697(3)	19.326(4)	20.207(2)	45.7351(15)	17.8124(6)
c/Å	13.520(2)	13.649(3)	11.4836(8)	27.2405(10)	25.002(1)
β/deg	110.14(2)	112.42(2)	94.434(7)	90	112.049(6)
V/Å ³	3191.0(9)	3001.7(12)	2769.2(4)	28101.9(17)	9416.6(8)
Z	2	2	2	4	4
d _{calc} /(g/cm ³)	1.398	1.463	1.489	1.320	1.370
abs coeff/ nm ⁻¹	0.72	0.76	0.82	1.25	0.94
F(000)	1404	1374	1300	11456	4016
cryst size/ mm	0.54 × 0.15 × 0.06	0.20 × 0.15 × 0.09	0.28 × 0.21 × 0.13	0.74 × 0.29 × 0.24	0.34 × 0.30 × 0.17
θ range/deg	3.4–29.6	3.4–29.4	3.4–28.2	3.4–29.6	3.3–29.5
limiting indices	h = -17 → 16, k = -25 → 27, l = -18 → 17	h = -16 → 15, k = -26 → 25, l = -17 → 18	h = -15 → 15, k = -26 → 25, l = -14 → 15	h = 0 → 30, k = 0 → 62, l = 0 → 36	h = -31 → 28, k = 0 → 24, l = 0 → 33
reflns coll'd/ unique	21901/7776	15770/7083	30572/6214	206873/35627	23378/23378
indep reflns/ R _{int}	5424/0.057	4048/0.079	5244/0.054	24347/0.109	17555/0.066
data/ restraints/ param	7776/0/388	7083/0/389	6214/62/353	35566/2549/1451	23376/2644/1099
GOF	0.92	1.00	0.92	1.08	0.92
R1, wR2 [I > 2σ(I)]	0.068, 0.207	0.069, 0.223	0.091, 0.243	0.141, 0.337	0.071, 0.225

Magnetic Measurements. Magnetic susceptibility data (2–300 K) were collected on powdered polycrystalline samples on a Quantum Design MPMS-XL SQUID magnetometer under an applied magnetic field of 0.1 T. Alternating-current (ac) measurements were performed in the 1.8–10 K range using 2.8 Oe ac field oscillation in the 1–1500 Hz range. Magnetization isotherms were collected at 2–5 K between 0 and 5 T. All data were corrected from the sample holder contribution, and the diamagnetism of the samples was estimated from Pascal's constants.¹⁴

Crystallography. A suitable crystal was selected and mounted on a Gemini κ geometry diffractometer (Agilent Technologies U.K. Ltd.) equipped with an Atlas CCD detector using Mo radiation (λ = 0.71073 Å). Intensities were collected at 100 K by means of the *CrysAlisPro* software.¹⁵ Reflection indexing, unit-cell parameter refinement, Lorentz polarization correction, peak integration, and background determination were carried out with the *CrysAlisPro* software.¹⁵ An analytical absorption correction was applied using the modeled faces of the crystal.¹⁶ The structures were solved by direct methods with *SIR97*, and the least-squares refinement on *F*² was achieved with the *CRYSTALS* software.¹⁷

All non-hydrogen atoms were refined anisotropically. The hydrogen atoms were all located in a difference map, but those attached to carbon atoms were repositioned geometrically. The hydrogen atoms were initially refined with soft restraints on the bond lengths and angles to regularize their geometry (C–H in the range 0.93–0.98 Å, N–H in the range 0.86–0.89 Å, and O–H = 0.82 Å) and *U*_{iso}(H) (in the range 1.2–1.5 times *U*_{eq} of the parent atom), after which the positions were refined with riding constraints. Data collection for single crystals of compounds 1–5 has been carried out at low temperature using an Xcalibur Atlas Gemini ultra diffractometer (for experimental details, see Table 1).

RESULTS AND DISCUSSION

Synthesis and Characterization. In a typical experiment, the family of polynuclear Co^{II}/ThiaSO₂ complexes was obtained by the solvothermal reaction of CoCl₂·4H₂O and ThiaSO₂ in a 10:1 (v/v) MeOH/H₂O mixed solvent with an amine-coordinating base such as pyridine or 1,2-diaminoethane. The compounds, designated as 1–5, were isolated in a highly crystalline form and fully characterized by a range of techniques, including X-ray diffraction (XRD), elemental analysis, FTIR, and mass spectrometry (MS). The solvent media for these types of reactions, leading to a polynuclear complex, may appear to be crucial. In fact, several types of polynuclear cobalt complexes with thiacalixarene ligands were obtained just with a change of solvent. For this reason, we have not changed the media parameter and kept the same MeOH/H₂O mixture over all syntheses.

Parameters such as the reaction time and metal/ligand ratio were screened and have allowed us to achieve the formation of a new family of compounds. Initially, the ratio metal/ligand was chosen as 2:1 and the heating time was studied. After 2 h of heating, a dinuclear complex, 1, is obtained, wherein ThiaSO₂ adopts a 1,2 alternate conformation. If chelating ligands such as 2,2'-bipyridine 2 or ethylenediamine 3 (which have a higher complexation constant for Co^{II} than pyridine) are used, even with long heating times, the dinuclear complexes obtained, 2 and 3, are stable and the ThiaSO₂ conformation is then locked. Contrarily, the heating of 1 results first, after 24 h of heating, in a mixture of the cobalt aggregate salt 4 and the neutral aggregate [Co₄(HThiaSO₂)₂(μ₃-H₂O)] (5) and then, after 1

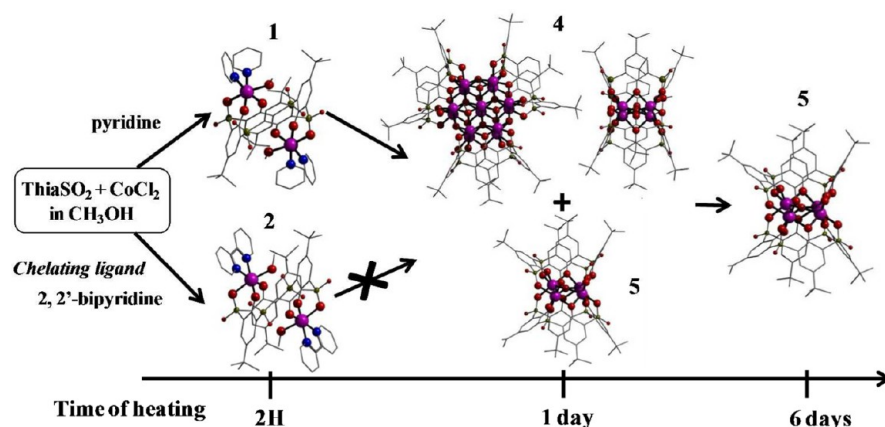


Figure 1. Reaction pathway leading to compounds 1, 2, 4, and 5. The representation of 1–5 arises from analysis by diffraction of the X-rays on a single crystal. Hydrogen atoms are omitted for clarity. Each atom is depicted as follows: Co, violet; S, yellow; O, red; C, gray; N, blue.

week of heating, finally in solely the neutral aggregate 5 (Figure 1). The formulas of 4 and 5 were confirmed by MS.

Upon 24 h of reaction, a mixture of compounds 4 and 5 is obtained with a majority of crystals 4. Varying the reaction parameters (temperature, Co^{II} /ThiaSO₂ ratio, etc.) did not allow us to quantitatively isolate phase 4. When the reaction time is raised to 48 h, a 50:50 mixture of phases 4 and 5 is obtained and the crystals of 4 display a pale-pink coating on the (010) and (100) faces of the crystals (Figure S1 in the SI). Finally, we managed to selectively isolate the neutral aggregate 5 by raising the reaction time to 6 days.

Structural Studies (1–3). A center of symmetry is located in the center of every molecule 1–3. Both cobalt ions present in 1–3 are thus exactly in the same octahedral environment consisting of two phenolic oxygen atoms, an oxygen atom of the sulfonyl group belonging to ThiaSO₂ and for 1 two pyridine and one methanol molecules, for 2 one molecule of 2,2'-bipyridine and one methanol molecules, and finally for 3 one 1,2-diaminoethane and one pyridine molecules (Figure 2 and Table 2).

This *fac*-tridentate mode [1.111] is the common coordination scheme of ThiaSO₂ with first-row transition-metal ions.

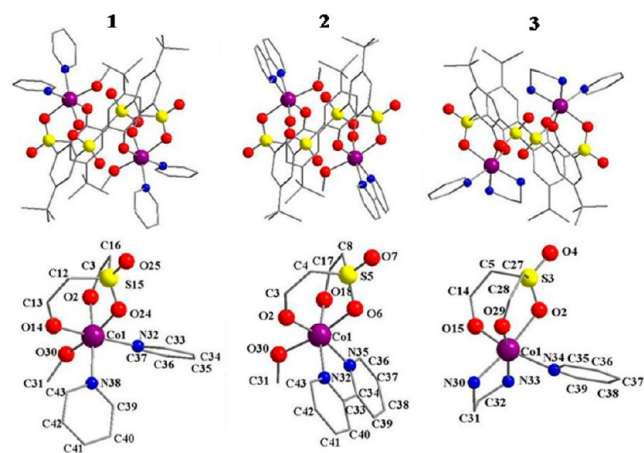


Figure 2. Structures arise from analysis by diffraction of the X-rays on a single crystal and ORTEP-type view of the cobalt environment of 1–3. Hydrogen atoms are omitted for clarity. Carbon is represented in wire/stick modes as gray. Each atom is depicted in standard “ball and stick” as follows: Co, violet; S, yellow; O, red; N, blue.

Table 2. Selected Bonds (Å) of 1–3

	1	2	3
Co1–O24	2.147(3)	Co1–O2	2.007(5)
Co1–O14	2.020(3)	Co1–O6	2.181(5)
Co1–O2	2.026(3)	Co1–O18	2.001(5)
Co1–O30	2.145(3)	Co1–O30	2.171(6)
Co1–N32	2.146(4)	Co1–N32	2.136(6)
Co1–N38	2.168(4)	Co1–N35	2.117(5)
Co1–Co1 ⁱ	5.7685(12)	Co1–Co1 ⁱ	5.6218(18)
		Co1–O29	2.017(4)
		Co1–O2	2.197(4)
		Co1–O15	2.040(4)
		Co1–N30	2.119(5)
		Co1–N33	2.165(5)
		Co1–N34	2.205(6)
		Co1–Co1 ⁱ	5.7132(9)

The distance between the two cobalt ions is on the order of 5.6–5.7 Å, which is relatively long for a possible magnetic interaction. In compounds 1 and 2, the methanol molecule points toward the two phenolic units. Finally, in each compound 1–3, the coordination sphere of each cobalt ion is a distorted octahedron.

For the molecule 3, the 1,2-diaminoethane ligand is directed to the phenolic units and steric hindrance allows coordination of a pyridine molecule rather than a methanol molecule. The values of the interatomic distances Co–O and Co–N, for the three compounds 1–3, are consistent for a II^+ oxidation state of the cobalt ion [bond-valence-sum (BVS) calculations].¹⁸

Compound 4. To our knowledge, $[\text{Co}_{14}][\text{Co}_4]$ 4 is the first polynuclear cobalt salt synthesized in a one-pot synthesis (Figure 3).

The anionic complex $[\text{Co}_4]$ has a common structure with those of the thialixarene complex family. This is a square of four Co^{II} ions sandwiched between two ThiaSO₂ macrocycles, as shown in Figure 3. In the middle of the square formed by the four Co^{II} ions, the presence of $\mu_4\text{-OH}^-$ gives a negative charge to the complex, which has been confirmed by MS. Four cobalt ions are seven-coordinated with capped trigonal-prismatic geometry. The Co–O distances are all on the order of 2.1 Å (Figure 4).

Charge balance is achieved by a cationic cluster $[\text{Co}_{14}]$ composed of 3 ThiaSO₂ ligands and 14 Co^{II} ions (Figures 4 and 5). $[\text{Co}_{14}]$ is formed by two superposed planar, body-centered, hexagonal cores formed by seven Co^{II} ions. Each heptanuclear wheel can be considered to be composed of six

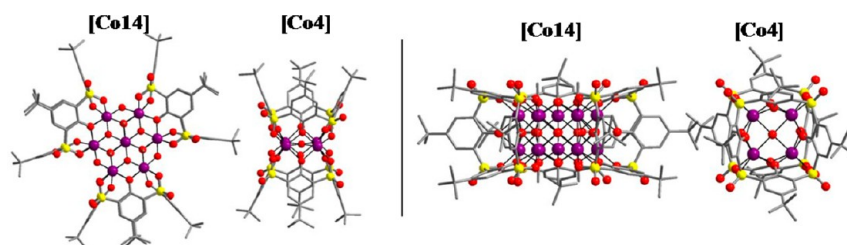


Figure 3. Two views of aggregate salt $[\text{Co}_{14}][\text{Co}_4]$ **4**. Hydrogen atoms are omitted for clarity. Carbon is represented in wire/stick mode as gray. Each atom is depicted in standard “ball and stick” as follows: Co, violet; S, yellow; O, red; N, blue.

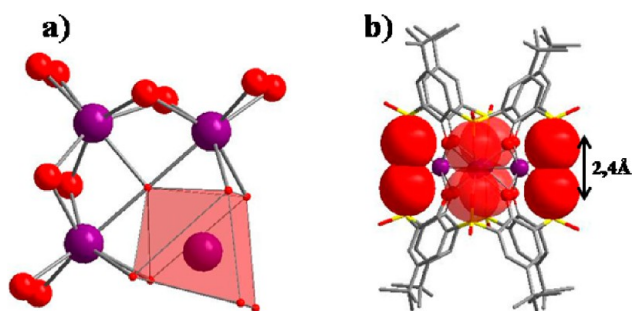


Figure 4. (a) Representation of four Co^{II} ions in capped trigonal prism. (b) Representation of oxygen atom interaction carried out by the axial sulfonyl groups. Carbon is represented in wire/stick mode as gray. Each atom is depicted as follows: Co, violet; O, red.

face-sharing monovalent distorted cubane units connected together by six vertices that are oxygen atoms (μ_6 ; Figure 5). The metallic core can also be described as two superimposed structures of Anderson–Evans type or as seven cells corresponding to the NiAs structure type, where the atoms of oxygen are in a compact hexagonal lattice and among which both octahedral sites are occupied by the Co^{II} ions.¹⁹ To the best of our knowledge, this topology of the $[\text{Co}_{14}]$ core is the first example in the literature, unlike the $[\text{M}_7]$ body-centered hexagonal topology, which is well-known for $\text{M} = \text{Zn}, \text{Co}, \text{Fe}, \text{Mn},$ and Ni .²⁰

In the MS spectrum recorded in negative mode, no peak corresponds to the calculated mass of m/z 3645. We find masses of m/z 3617, 3603, 3589 and 3575, which correspond to the partial substitution of the methanolato groups by hydroxo groups. For example, the mass of m/z 3617 corresponds to hydrolysis of two CHO groupings of six (Figures S8 and S9 in the SI). Each of the 14 cobalt ions is in a pseudooctahedral coordination environment. ThiaSO₂ molecules in the cone conformation cap three hexagonal faces of the core. The Co–O distance lies between 2 and 2.2 Å, which is in

agreement with a $\text{II}+$ oxidation state for the cobalt atoms as calculated using bond valence theory.¹⁸

The molecular structure of **5** consists of two molecules of ThiaSO₂ sandwiching four cobalt ions (Figure 6a). Both ThiaSO₂ molecules are in the pinched cone conformation [$d(\text{C}49-\text{C}40)/d(\text{C}56-\text{C}28) = 0.57$ and $d(\text{C}104-\text{C}92)/d(\text{C}84-\text{C}113) = 0.7$]. Each Co^{II} ion is six-coordinated and possesses a different geometry environment. Co5 can be considered as being in trigonal-prismatic coordination, Co4 and Co1 in deformed octahedral coordination, and Co2 in octahedral coordination (Figure 6).

Anions $[\text{Co}_4]$ in compounds **4** and **5** are similar, and their structures are closely related, as presented in Figure 7. It seems possible to pass from one complex to the other by a twist of the ThiaSO₂ macrocycle relative to the plane formed by the cobalt ions. The O3 atom (Figure 6a) is most probably a hydroxo group (BVS calculations). In this case, one of the oxygen atoms from the phenolato group has to be protonated to achieve the neutral charge of compound **5**. This hypothesis is confirmed by MS. Indeed, it seems easier to remove a proton from the phenolato group rather than from a water molecule if the O3 atom belongs to a water molecule. The strong interaction between axial oxygen atoms (2.4 Å, while the O–O van der Waals bond is around 2.9 Å) carried out by the sulfonyl groups of the anion $[\text{Co}_4]$ in compound **4**, and protonation of one phenolato group, is certainly the cause of this transformation (Figure 4b): distortion observed during the passage of trigonal-prismatic geometry to an octahedral geometry around the metallic ions.²¹ In a previous paper, we have reported substitution of the $\mu_4\text{-OH}^-$ group by an anion $\mu_4\text{-F}^-$ in a tetranuclear manganese(II) complex isostructural to the anion $[\text{Co}_4]$ in compound **4**.^{9f} Similarly, we were able to substitute the OH group by a fluorine atom in the cobalt complex. This seems to stabilize the complex because the reaction time (2, 3, and 6 days) always led to the same compound. This was confirmed by MS in negative mode, which indicates a mass of m/z 1943 corresponding to the raw formula $\text{C}_{80}\text{H}_{88}\text{O}_{24}\text{S}_8\text{F}_1\text{Co}_4$

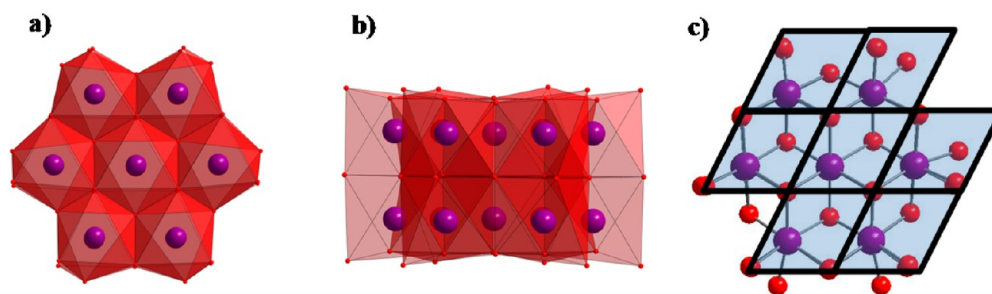


Figure 5. (a and b) Two views of the $[\text{Co}_{14}]$ core topology. (c) Projection of the compact hexagonal cell. Each atom is depicted in standard “ball and stick” as follows: Co, violet; O, red.

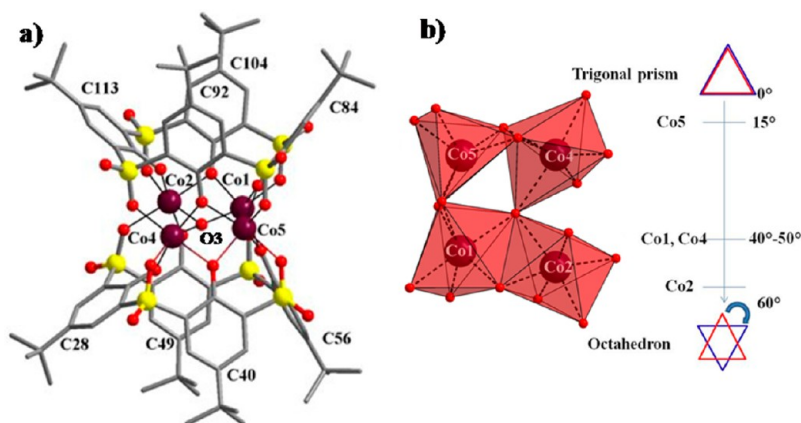


Figure 6. (a) View of aggregate 5. Hydrogen atoms are omitted for clarity. Each atom is depicted in standard “ball and stick” as follows: C, gray; Co, violet; S, yellow; O, red; N, blue. (b) Representation of the environment of the four cobalt ions in compound 5.

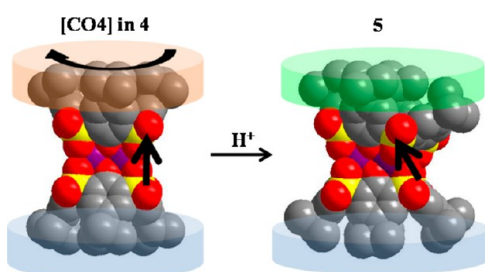


Figure 7. Possible family ties between the anion $[\text{Co}_4]$ in 4 and compound 5 by rotation of one ThiaSO₂.

and confirms substitution of the $\mu_4\text{-OH}^-$ by a $\mu_4\text{-F}^-$ anion 4 (Figure S11 in the SI). In positive mode, the spectrum is identical with that obtained for cation 4. Thereby, in the case of anion $[\text{Co}_4]$, it appears that when the $\mu_4\text{-OH}^-$ group is substituted by the $\mu_4\text{-F}^-$ anion, protonation of the phenolato group is not possible in this condition and the $[\text{Co}_4]$ anion is stable.

Magnetic Measurements. Magnetic studies of both direct current (dc) and ac were performed on all five compounds. The χT product of quasi-planar (with planar arrangements of four Co^{II} ions) tetranuclear clusters 5 (Figure 8) at 300 K is 13.47 $\text{cm}^3/\text{K}\cdot\text{mol}$, which is typical for four uncoupled Co^{II} ions but larger than that for four free $S = 3/2$ spins ($\chi T = 7.50 \text{ cm}^3/\text{K}\cdot\text{mol}$ and $g = 2.0$) as a result of the presence of a significant

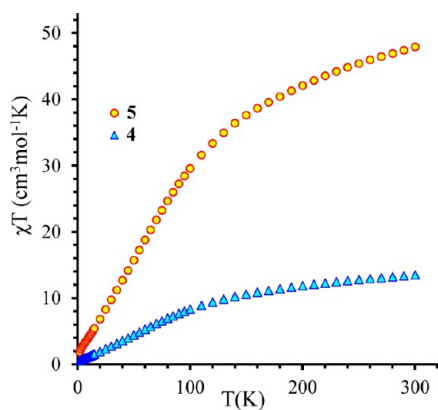


Figure 8. Temperature dependence of the χT product for compounds 4 and 5 at $H_{\text{dc}} = 0.1 \text{ T}$.

spin–orbital contribution in the susceptibility of octahedral high-spin Co^{II} .^{5,22} A gradual decrease of χT is observed with temperature, and χT reaches a value of 0.52 $\text{cm}^3/\text{K}\cdot\text{mol}$ at 2 K (Figure 8). In the case of clusters containing octahedral Co^{II} ions, the decrease of χT at low temperature can be an effect of an important spin–orbital contribution and also a dominant antiferromagnetic interaction between four paramagnetic centers.

The value of χT at low temperature is too low for four noncoupling Co^{II} paramagnetic centers and suggests the presence of antiferromagnetic interaction between four paramagnetic centers. The presence of a dominant antiferromagnetic interaction is also confirmed by magnetization measurements at 2–5 K. Magnetization does not saturate at the high-field limit (5 T) of our instrument. The experimental value of magnetization at 2.0 K and 5 T is 1.60 $N\beta$, which is too low for four noncoupled Co^{II} ions (Figure S5 in the SI).

According to X-ray investigation compound 4 is composed of anionic $[\text{Co}_4]$ and cationic $[\text{Co}_{14}]$ clusters. The anionic tetranuclear $[\text{Co}_4]$ species contains seven-coordinated Co^{II} paramagnetic centers, and the cationic Co_{14} cluster contains six-coordinated Co^{II} paramagnetic centers. On the basis of BVS analysis, all cobalt centers correspond to the 2+ oxidation state. The susceptibility data for 4 are plotted as χT versus T , as depicted in Figure 8.

With decreasing temperature (300 to 2 K), the χT product decreases progressively from 47.9 $\text{cm}^3/\text{K}\cdot\text{mol}$ to reach 1.85 $\text{cm}^3/\text{K}\cdot\text{mol}$ at 2 K. Similar to 5, drastic modification of the susceptibility with temperature can be associated with the presence of an important spin–orbital contribution and a dominant antiferromagnetic interaction in 4. This conclusion is consistent with magnetization measurements presented in the form of the H versus T plot (Figure S6a in the SI) and reduced magnetization plot (Figure S6b in the SI).

The dynamic properties of compounds 4 and 5 have been investigated using ac susceptibility measurements as a function of the temperature at different frequencies and also at different temperatures as a function of the frequency at 2.8 Oe field oscillating between 1 and 1500 Hz. Compounds 4 and 5 did not show any out-of-phase signal at zero dc magnetic field. No modifications in the out-of-phase susceptibility after application of the dc magnetic field (0–3.0 T) are detected.

The dc experiment at 0.1 T in the temperature range 2–300 K was performed also for the series of dinuclear $\text{Co}^{\text{II}}/\text{ThiaSO}_2$ -bridged compounds 1–3 (Figure 9).

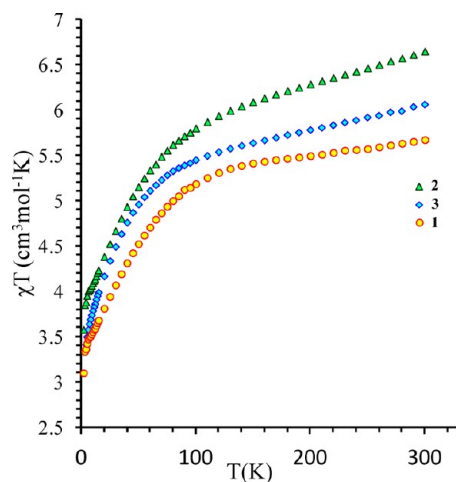


Figure 9. Temperature dependence of the χT product at $H_{dc} = 0.1$ T for compounds 1–3.

The product of χT at 300 K has values of 5.67, 6.06, and 6.65 $\text{cm}^3/\text{K}\cdot\text{mol}$, respectively, for 1–3 and is larger than the expected spin-only value for two high-spin isolated Co^{II} ions ($S = 3/2$ of 3.75 $\text{cm}^3/\text{K}\cdot\text{mol}$ and $g = 2.00$), indicating an important spin–orbital contribution (Figure 10). At the beginning, the product of χT slowly decreases and after 70 K drops off to reach values of 3.10 $\text{cm}^3/\text{K}\cdot\text{mol}$ for 1, 3.58 $\text{cm}^3/\text{K}\cdot\text{mol}$ for 2, and 3.85 $\text{cm}^3/\text{K}\cdot\text{mol}$ for 3 at 2 K. This behavior suggests the presence of a zero-field-splitting (ZFS) component in the magnetic susceptibility or a strong antiferromagnetic interaction in the 1–3 dinuclear series. Because of the absence of common bridging functions (Figure 2 and Table 2) and large distances between Co^{II} paramagnetic centers (around 5.7 Å), their magnetic interaction is likely insignificant. When the magnetic interaction between Co^{II} ions is neglected, the temperature dependence of χT in the range of 10–300 K can be described in terms of two isolated Co^{II} ions.

Octahedral coordination polyhedra in 1–3 have slightly different distortion, implying differences in the ZFS parameters and g tensors with respective impact on the magnetic properties. The dynamic properties of the three compounds

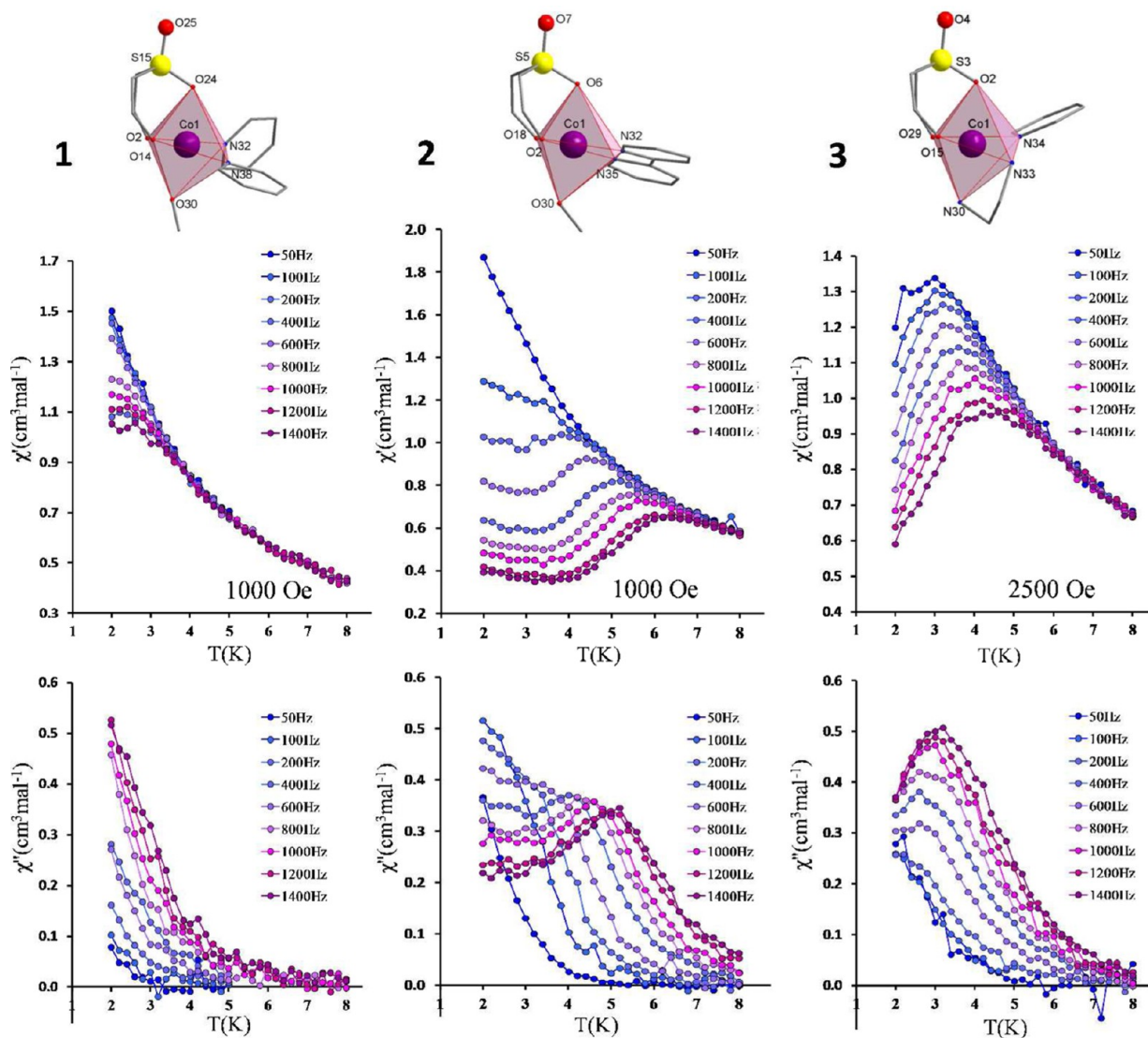


Figure 10. Temperature dependence of the in-phase (χ') and out-of-phase (χ'') ac susceptibility frequency components for 1–3 at the indicated applied dc field.

1–3 were investigated using temperature- and frequency-dependent ac susceptibility measurements at 2.7 Oe field oscillating between 50 and 1500 Hz. For the three compounds under a zero dc field, no ac signal was observed in the temperature range of 2–10 K.

Applying a small magnetic field clearly shows the appearance of a nonzero out-of-phase signal χ'' in ac measurement (Figure 10) with a strong frequency dependence in the case of all three compounds.

Such behavior usually indicates that a slow relaxation of the magnetization can be a result of quantum tunneling of the magnetization (QTM) through the spin-reversal barrier via degenerate $\pm M_s$ energy levels, as observed previously in the case of Co^{II} and Fe^{II} SIM,²³ of transverse anisotropy barrier governed by E instead of D ,³⁰ or of an optical acoustic Raman process.²⁶

The anisotropic barrier energies U_{eff} are obtained from temperature (Figure 10) and frequency sweeping measurements (Figure S7 in the SI). The effective energy barriers obtained from the fitting procedure according the Arrhenius law are $U_{\text{eff}}(2) = 10.7 \text{ K}$ ($\tau_0 = 4.02 \times 10^{-6}$) for 2 and $U_{\text{eff}}(3) = 20.3 \text{ K}$ ($\tau_0 = 2.24 \times 10^{-6}$) for 3 (Figure 11). Assuming $S = 3/2$,

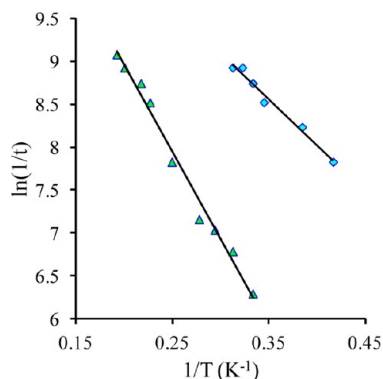


Figure 11. Arrhenius plots for 3 (\diamond) and 2 (\triangle).

the ZFS parameters can be estimated from equation²⁴ $U_{\text{eff}} = (S^2 - 1/4)|D|$ and have values of $|D| = 5.3 \text{ K}$ for 2 and 10.1 K for 3. To quantify the ZFS parameters, magnetization data (0–5 T) of 1–3 were fitted to the Hamiltonian $H = DS_z^2 + E(S_x^2 + S_y^2) + g_{\text{iso}}\mu_B\mathbf{S}\mathbf{B}$ using ANISOFIT software.²⁵ The symbol μ_B represents the Bohr magneton; D , E , S , and \mathbf{B} stand for the axial and rhombic ZFS parameters and the spin and magnetic field vectors, respectively. The best fits are presented in Figure 12 and correspond to the positive values of ZFS: $D = +15.31 \text{ cm}^{-1}$, $g_{\text{iso}} = 2.27$; $D = +21.50 \text{ cm}^{-1}$, $g_{\text{iso}} = 2.51$; $D = +18.20 \text{ cm}^{-1}$, $g_{\text{iso}} = 2.40$ respectively for 1–3. Similar to this work, additional reported examples of cobalt(II) complexes with positive D values can exhibit slow relaxation of magnetization.^{26–30} The presence of slow relaxation can be ascribed to a field-induced Orbach relaxation pathway,²⁷ a transverse anisotropy barrier governed by E instead of D ,³⁰ or an optical acoustic Raman process, which can have an important influence in magnetic relaxation.²⁶ The presence of different contributions to the relaxation process probably originates from a discrepancy between ZFS parameters estimated for relaxation processes and magnetization measurements; especially, this discrepancy was recently reported^{29–32} in the case of mononuclear Co^{II} SIMs. In our case, analysis of magnetic data can be further affected by the presence of small magnetic interaction between two Co^{II} ions.

CONCLUSION

We have synthesized and characterized five new cobalt(II) clusters (1–5) bridged by thiacalixarene ligands. All of these complexes are of particular interest in the field of synthetic chemistry as well as magnetic materials. Through a change in the heating time during the reaction process, an association between the different complexes has been demonstrated. The addition of chelating ligands was shown to be a critical factor for stabilization of the two dinuclear complexes 2 and 3. On the other hand, if the ligand used is nonchelating, the dinuclear complexes show instability over time, leading to the formation of compounds 4 and 5. Each step of the transformation process has been optimized and globally understood. The

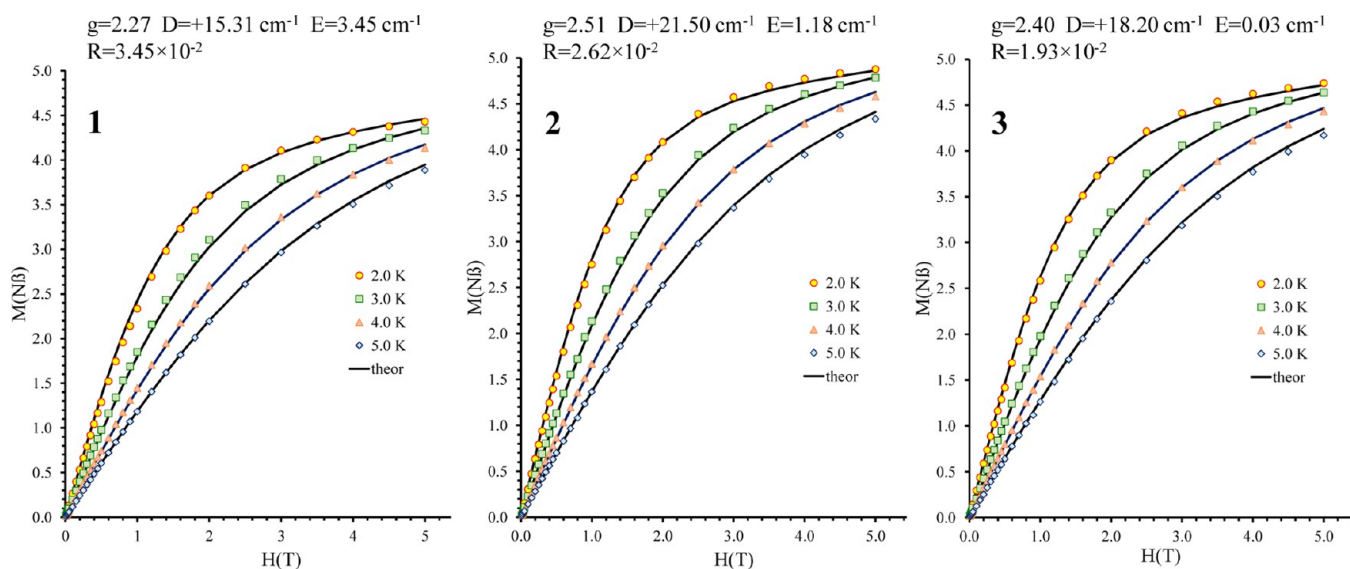


Figure 12. Magnetization data collected on microcrystalline compounds 1–3 at different temperatures and dc fields. Black lines correspond to the best fits with ANISOFIT 2.0 with $S = 3/2$.

sulfonylcalix[4]arene ligand has shown a great adaptability to the metallic ion coordination sphere because of its ability to adopt different conformational states. Thus, a strong link existing between the ThiaSO₂ ligand and the Co^{II} coordination sphere confirms its utility as a terminal ligand and allows one to consider its use for the achievement of other types of original aggregates. We plan to further investigate the impact of other synthetic parameters on the obtained systems such as the stoichiometric ratio or pH modulation. The dinuclear compounds 1–3 containing two encapsulated Co^{II} ions show a slow magnetization relaxation in the presence of an applied dc field. The ZFS parameters, quantified from magnetization data, were found to have moderate magnitude and positive values. The origin of positive ZFS arises from strong octahedral distortion and particular effects of the thialixarene, pyridine, bipyridine, ethylenediamine, and methanol donor atoms (nitrogen and oxygen). Further studies are currently ongoing regarding the influence of other chelating ligands, in order to investigate their influence on the coordination sphere of the metallic ion and magnetic properties of the complexes.

■ ASSOCIATED CONTENT

📄 Supporting Information

Faces of a crystal of **4**, view in compact mode of the compound, field dependence of the magnetization of **5** at the indicated temperatures, SM field dependence of the magnetization of **4** at the indicated temperatures, SM field dependence of magnetization of **4** as a plot of M versus H/T at indicated temperatures, and the best fits of variable-temperature $\chi_M T$ data for **3** and **2**. The structures have been deposited with the Cambridge Crystallographic Data Center as CCDC 873249 for **1**, 873255 for **2**, and 881987 for **3** and can be obtained, upon request, from the Director, Cambridge Crystallographic Data Centre, 12 Union Road, Cambridge CB2 1EZ, U.K. This material is available free of charge via the Internet at <http://pubs.acs.org>.

■ AUTHOR INFORMATION

Corresponding Author

*E-mail: cedric.desroches@univ-lyon1.fr.

Notes

The authors declare no competing financial interest.

■ ACKNOWLEDGMENTS

The structure measurements were performed at the “Centre de Diffraction Longchambon” of the University of Lyon. We thank F. Albrieux, C. Duchamp, and N. Henriques from the “Centre Commun de Spectrométrie de Masse” (ICBMS UMR-5246) for the assistance and access to the Mass Spectrometry facilities.

■ REFERENCES

- (1) Gatteschi, D.; Sessoli, R.; Villain, J. *Molecular Nanomagnets*; Oxford University Press: Oxford, U.K., 2006.
- (2) (a) Sessoli, R.; Gatteschi, D.; Caneschi, A.; Novak, M. *Nature* **1993**, *365*, 141. (b) Sessoli, R.; Tsai, H.-L.; Schake, A. R.; Wang, S.; Vincent, J. B.; Folting, K.; Gatteschi, D.; Christou, G.; Hendrickson, D. N. *J. Am. Chem. Soc.* **1993**, *115*, 1804. (c) Milios, C. J.; Vinslava, A.; Wernsdorfer, W.; Moggach, S.; Parsons, S.; Perlepes, S. P.; Christou, G.; Brechin, E. K. *J. Am. Chem. Soc.* **2007**, *129*, 2754. (d) Bagai, R.; Christou, G. *Chem. Soc. Rev.* **2009**, *38*, 1011.
- (3) Neese, F.; Pantazis, D. A. *Faraday Discuss.* **2011**, *148*, 229.
- (4) Murrie, M. *Chem. Soc. Rev.* **2010**, *39*, 1986.

(5) Lloret, F.; Julve, M.; Cano, J.; Ruiz-Garcia, R.; Pardo, E. *Inorg. Chim. Acta* **2008**, *361*, 3432.

(6) See, for example: (a) Lydon, C.; Sabi, M. M.; Symes, M. D.; Long, D. L.; Murrie, M.; Yoshii, S.; Nojiri, H.; Cronin, L. *Chem. Commun.* **2013**, *48*, 9819. (b) Galloway, K. W.; Schmidtman, M.; Sanchez-Benitez, J.; Kamenev, K. V.; Wernsdorfer, W.; Murrie, M. *Dalton Trans.* **2010**, *39*, 4727. (c) Ibrahim, M.; Lan, Y. H.; Bassil, B. S.; Xiang, Y. X.; Suchopar, A.; Powell, A. K.; Kortz, U. *Angew. Chem., Int. Ed.* **2011**, *50*, 4708. (d) Klower, F.; Lan, Y.; Nehrkorn, J.; Waldmann, O.; Anson, C. E.; Powell, A. K. *Chem.—Eur. J.* **2009**, *15*, 7413. (e) Pattacini, R.; Teo, P.; Zhang, J.; Lan, Y. H.; Powell, A. K.; Nehrkorn, J.; Waldmann, O.; Hor, T. S. A.; Braunstein, P. *Dalton Trans.* **2011**, *40*, 10526. (f) Kostakisa, G. E.; Perlepes, S. P.; Blatov, V. A.; Proserpiod, D. M.; Powell, A. K. *Coord. Chem. Rev.* **2012**, *256*, 1246. (g) Chibotaru, L. F.; Ungur, L. F.; Aronica, C.; Elmoll, H.; Pilet, G.; Luneau, D. *J. Am. Chem. Soc.* **2008**, *130*, 12445. (h) Brechin, E. K.; Graham, A.; Parkin, A.; Parsons, S.; Seddon, A. M.; Winpenny, R. E. P. *J. Chem. Soc., Dalton Trans.* **2000**, 3242. (i) Langley, S.; Helliwell, M.; Sessoli, R.; Teat, S. J.; Winpenny, R. E. P. *Inorg. Chem.* **2008**, *47*, 497. (j) Wu, D.; Guo, D.; Song, Y.; Huang, W.; Duan, C.; Meng, Q.; Sato, O. *Inorg. Chem.* **2009**, *48*, 854. (k) Langley, S. J.; Helliwell, M.; Sessoli, R.; Rosa, P.; Wernsdorfer, W.; Winpenny, R. E. P. *Chem. Commun.* **2005**, 5029. (l) Murrie, M.; Teat, S. J.; Stoeckli-Evans, H.; Gudel, H. U. *Angew. Chem., Int. Ed.* **2003**, *42*, 4653.

(7) (a) Winpenny, R. E. P. *J. Chem. Soc., Dalton Trans.* **2002**, 1. (b) Tasiopoulos, A. J.; Perlepes, S. P. *Dalton Trans.* **2008**, 5537.

(8) Roesky, H. W.; Haiduc, L.; Hosmane, N. S. *Chem. Rev.* **2003**, *103*, 2579.

(9) For thialixarene, see, for example: (a) Kajiwara, T.; Iki, N.; Yamashita, M. *Coord. Chem. Rev.* **2007**, *251*, 1734. (b) Desroches, C.; Pilet, G.; Borshch, S. A.; Parola, S.; Luneau, D. *Inorg. Chem.* **2005**, *44*, 9112. (c) Desroches, C.; Pilet, G.; Szilagyi, P. Á.; Molnar, G.; Borshch, S. A.; Bousseksou, A.; Parola, S.; Luneau, D. *Eur. J. Inorg. Chem.* **2006**, *2*, 357. (d) Mislin, G.; Graf, E.; Hosseini, M. W.; Bilyk, A.; Hall, A. K.; Harrowfield, J. M.; Skelton, B. W.; White, A. H. *Chem. Commun.* **1999**, 373. (e) Akdas, H.; Graf, E.; Hosseini, M. W.; De Cian, A.; Bilyk, A.; Skelton, B. W.; Koutsantonis, G. A.; Murray, I.; Harrowfield, J. M.; White, A. H. *Chem. Commun.* **2002**, 1042. (f) Lamouchi, M.; Jeanneau, E.; Brioude, A.; Pillonnet, A.; Martini, M.; Stéphane, O.; Meganem, F.; Novitchi, G.; Luneau, D.; Desroches, C. *Dalton Trans.* **2012**, *41*, 2707. (g) Bi, Y.; Wang, X.; Liao, W.; Wang, X.; Deng, R.; Zhang, H.; Gao, S. *J. Am. Chem. Soc.* **2009**, *131*, 11650. (h) Gehin, A.; Ferlay, S.; Harrowfield, J. M.; Fenske, D.; Kyritsakas, N.; Hosseini, M. W. *Inorg. Chem.* **2012**, *51*, 5481. (i) Bi, Y.; Duab, S.; Liao, W. *Chem. Commun.* **2011**, *47*, 4724. (j) Kajiwara, T.; Kobashi, T.; Shinagawa, R.; Ito, T.; Takaishi, S.; Yamashita, M.; Iki, N. *Eur. J. Inorg. Chem.* **2006**, 1765. (k) Xiong, K.; Jiang, F.; Gai, Y.; He, Z.; Yuan, D.; Chen, L.; Su, K.; Hong, M. *Cryst. Growth Des.* **2012**, *12*, 3335. (l) Bi, Y.; Liao, W.; Xu, G.; Deng, R.; Wang, M.; Wu, Z.; Gao, S.; Zhang, H. *Inorg. Chem.* **2010**, *49*, 7735. (m) Kajiwara, T.; Yokozawa, S.; Ito, T.; Iki, N.; Morohashi, N.; Miyano, S. *Chem. Lett.* **2001**, 6.

(10) For calixarene, see, for example: (a) Karotsis, G.; Teat, S. J.; Wernsdorfer, W.; Piligkos, S.; Scott, J. D.; Brechin, E. K. *Angew. Chem., Int. Ed.* **2009**, *48*, 8285. (b) Karotsis, G.; Evangelisti, M.; Dalgarno, S. J.; Brechin, E. K. *Angew. Chem., Int. Ed.* **2009**, *48*, 9928. (c) Karotsis, G.; Kennedy, S.; Dalgarno, S. J.; Brechin, E. K. *Chem. Commun.* **2010**, *46*, 3884. (d) Taylor, S. M.; McIntosh, R. D.; Piligkos, S.; Dalgarno, S. J.; Brechin, E. K. *Chem. Commun.* **2012**, *48*, 11190. (e) Taylor, S. M.; McIntosh, R. D.; Beavers, C. M.; Teat, S. J.; Piligkos, S.; Dalgarno, S. J.; Brechin, E. K. *Chem. Commun.* **2011**, *47*, 1440. (f) Karotsis, G.; Kennedy, S.; Teat, S. J.; Beavers, C. M.; Fowler, D. A.; Morales, J. J.; Evangelisti, M.; Dalgarno, S. J.; Brechin, E. K. *J. Am. Chem. Soc.* **2010**, *132*, 12983. (g) Aronica, C.; Chastanet, G.; Zueva, E.; Borshch, S. A.; Clemente-Juan, J. M.; Luneau, D. *J. Am. Chem. Soc.* **2008**, *130*, 2365. (h) Taylor, S. M.; Karotsis, G.; McIntosh, R. D.; Kennedy, S.; Teat, S. J.; Beavers, C. M.; Wernsdorfer, W.; Piligkos, S.; Dalgarno, S. J.; Brechin, E. K. *Chem.—Eur. J.* **2011**, *17*, 7521. (i) Taylor, S. M.; Sanz, S.; McIntosh, R. D.; Beavers, C. M.; Teat, S. J.; Brechin, E. K.; Dalgarno, S. J. *Chem.—Eur. J.* **2012**, *18*, 16014. (j) McLellan, R.;

Kennedy, K. M.; Denis, M.; McIntosh, R. D.; Brechin, E. K.; Dalgarno, S. J. *Polyhedron* **2013**, *55*, 126.

(11) Synthesis of thiacalixarene: (a) Kumagai, H.; Hasegawa, M.; Miyanari, S.; Sugawa, Y.; Sato, Y.; Hori, T.; Ueda, S.; Kamiyama, H.; Miyano, S. *Tetrahedron Lett.* **1997**, *38*, 3971. (b) Morohashi, N.; Narumi, F.; Iki, N.; Hattori, T.; Miyano, S. *Chem. Rev.* **2006**, *106* (12), 5291.

(12) (a) Bilyk, A.; Dunlop, J. W.; Fuller, R. O.; Hall, A. K.; Harrowfield, J. M.; Hosseini, M. W.; Koutsantonis, G. A.; Murray, I. W.; Skelton, B. W.; Sobolev, A. N.; Stamps, R. L.; White, A. H. *Eur. J. Inorg. Chem.* **2010**, 2106. (b) Morohashi, N.; Hattori, T.; Yokomakura, K.; Kabuto, C.; Miyano, S. *Tetrahedron Lett.* **2002**, *43*, 7769. (c) Buccella, D.; Parkin, G. J. *Am. Chem. Soc.* **2008**, *130*, 8617. (d) Kajiwara, T.; Yokozawa, S.; Ito, T.; Iki, N.; Morohashi, N.; Miyano, S. *Angew. Chem., Int. Ed.* **2002**, *41*, 2076.

(13) Coxall, R. A.; Harris, S. G.; Henderson, D. K.; Parsons, S.; Tasker, P. A.; Wimpenny, R. E. P. *J. Chem. Soc., Dalton Trans.* **2000**, 2349.

(14) Pascal, P. *Ann. Chim. Phys.* **1910**, *19*, 5.

(15) *CrysAlisPro*, version 1.171.34.49; Agilent Technologies: Santa, CA (release 20-01-2011 *CrysAlis171.NET*) (compiled Jan 20, 2011, 15:58:25).

(16) Clark, R. C.; Reid, J. S. *Acta Crystallogr.* **1995**, *A51*, 887.

(17) (a) Altomare, A.; Burla, M. C.; Camalli, M.; Cascarano, G. L.; Giacovazzo, C.; Guagliardi, A.; Moliterni, A. G. G.; Polidori, G.; Spagna, R. *J. Appl. Crystallogr.* **1999**, *32*, 115. (b) Betteridge, P. W.; Carruthers, J. R.; Cooper, R. I.; Prout, K.; Watkin, D. J. *J. Appl. Crystallogr.* **2003**, *36*, 1487.

(18) Wood, R. M.; Palenik, G. J. *Inorg. Chem.* **1998**, *37*, 4149.

(19) Evans, H. T. *Acta Crystallogr., Sect. B* **1974**, *10*, 2095.

(20) For example, see: (a) Alley, K. G.; Bircher, R.; Waldmann, O.; Ochsenbein, S. T.; Güdel, H. U.; Moubaraki, B.; Murray, K. S.; Fernandez-Alonso, F.; Abrahams, B. F.; Boskovic, C. *Inorg. Chem.* **2006**, *45*, 8950. (b) Koizumi, S.; Nihei, M.; Shiga, T.; Nakano, M.; Nojiri, H.; Bircher, R.; Waldmann, O.; Ochsenbein, S. T.; Güdel, H. U.; Fernandez-Alonso, F.; Oshio, H. *Chem.—Eur. J.* **2007**, *13*, 8445. (c) Oshio, H.; Hoshino, N.; Ito, T.; Nakano, M.; Renz, F.; Gutlich, P. *Angew. Chem., Int. Ed.* **2003**, *42*, 223. (d) Tesmer, M.; Müller, B.; Vahrenkamp, H. *Chem. Commun.* **1997**, 721. (e) Meally, S. T.; Karotsis, G.; Brechin, E. K.; Papaefstathiou, G. S.; Dunne, P. W.; McArdle, P.; Jones, L. F. *CrystEngComm* **2010**, *12*, 59. (f) Meally, S. T.; McDonald, C.; Karotsis, G.; Papaefstathiou, G. S.; Brechin, E. K.; Dunne, P. W.; McArdle, P.; Power, N. P.; Jones, L. F. *Dalton Trans.* **2010**, 39, 4809. (g) Meally, S. T.; McDonald, C.; Kealy, P.; Taylor, S. M.; Brechin, E. K.; Jones, L. F. *Dalton Trans.* **2012**, *41*, 5610. (h) Ferguson, A.; Parkin, A.; Sanchez-Benitez, J.; Kamenev, K.; Wernsdorfer, W.; Murrie, M. *Chem. Commun.* **2007**, 3473.

(21) Eisenberg, R.; Ibers, J. A. *Inorg. Chem.* **1966**, *5*, 411.

(22) Kahn, O. *Molecular Magnetism*; VCH Publishers, Inc.: New York, 1993.

(23) (a) Cremades, E.; Ruiz, E. *Inorg. Chem.* **2011**, *50*, 4016. (b) Gomez-Coca, S.; Cremades, E.; Aliaga-Alcalde, N. R.; Ruiz, E. J. *Am. Chem. Soc.* **2013**, *135*, 7010. (c) Atanasov, M.; Zadrozny, J. M.; Long, J. R.; Neese, F. *Chem. Sci.* **2013**, *4*, 139. (d) Zadrozny, J. M.; Atanasov, M.; Bryan, A. M.; Lin, C. Y.; Rekken, B. D.; Power, P. P.; Neese, F.; Long, J. R. *Chem. Sci.* **2013**, *4*, 125. (e) Zadrozny, J. M.; Long, J. R. *J. Am. Chem. Soc.* **2011**, *133*, 20732. (f) Harman, W. H.; Harris, T. D.; Freedman, D. E.; Fong, H.; Chang, A.; Rinehart, J. D.; Ozarowski, A.; Sougrati, M. T.; Grandjean, F.; Long, G. J.; Long, J. R.; Chang, C. J. *J. Am. Chem. Soc.* **2010**, *132*, 18115. (g) Rinehart, J. D.; Long, J. R. *Chem. Sci.* **2010**, *2*, 2078.

(24) (a) Jurca, T.; Farghal, A.; Lin, P.-H.; Korobkov, I.; Murugesu, M.; Richeson, D. S. *J. Am. Chem. Soc.* **2011**, *133*, 15814. (b) Long, J. R. *Chem. Commun.* **2012**, *48*, 3897.

(25) Shores, M. P.; Sokol, J. J.; Long, J. R. *J. Am. Chem. Soc.* **2002**, *124*, 2279.

(26) Colacio, E.; Ruiz, J.; Ruiz, E.; Cremades, E.; Krzystek, J.; Carretta, S.; Cano, J.; Guidi, T.; Wernsdorfer, W.; Brechin, E. K. *Angew. Chem., Int. Ed.* **2013**, *52*, 9130.

(27) Zadrozny, J. M.; Liu, J.; Piro, N. A.; Chang, C. J.; Hill, S.; Long, J. R. *Chem. Commun.* **2012**, *48*, 3927.

(28) Gomez-Coca, S.; Cremades, E.; Aliaga-Alcalde, N.; Ruiz, E. J. *Am. Chem. Soc.* **2013**, *135*, 7010.

(29) Zadrozny, J. M.; Telsler, J.; Long, J. R. *Polyhedron* **2013**, *64*, 209.

(30) Vallejo, J.; Castro, I.; Ruiz-García, R.; Cano, J.; Julve, M.; Lloret, F.; De Munno, G.; Wernsdorfer, W.; Pardo, E. *J. Am. Chem. Soc.* **2012**, *134*, 15704.

(31) Buchholz, A.; Eseola, A. O.; Plass, W. C. R. *Chimie* **2012**, *15*, 929.

(32) Cangussu, D.; Pardo, E.; Dul, M.-C.; Lescouëzec, R.; Herson, P.; Journaux, Y.; Pedrosa, E. F.; Pereira, C. L. M.; Stumpf, H. O.; Carmen Muñoz, M.; Ruiz-García, R.; Cano, J.; Julve, M.; Lloret, F. *Inorg. Chim. Acta* **2008**, *361*, 3394.